INTERNATIONAL SOCIETY FOR SOIL MECHANICS AND GEOTECHNICAL ENGINEERING

SIMSG   ISSMGE

A practical study on the induced seismicity in Groningen and the seismic response of a masonry structure

S. Panagoulias[1], A. Laera[1] & R.B.J. Brinkgreve[1,2]
[1] Plaxis bv, Delft, the Netherlands
[2] Faculty of Civil Engineering and Geosciences – Delft University of Technology, Delft, the Netherlands

ABSTRACT

In this paper the man-induced earthquakes in Groningen (the Netherlands) are studied in terms of site response analyses and liquefaction evaluation. A particular soil profile in Loppersum is employed and soil properties are determined based on available geotechnical data. Clayey soil layers are modelled by means of the Generalised Hardening Soil (GHS) model. Sandy soil layers are modelled either with the GHS model or with the UBC3D-PLM model, depending on the purpose of the analysis. The UBC3D-PLM model is used to assess the liquefaction potential. Numerical results are verified against analytical formulations. The non-linear site response of the relatively soft soil deposit is captured well by PLAXIS. Special focus is given to a practical application, considering the response of a shallow-founded masonry structure under seismic excitation. The masonry is simulated by means of the Jointed Rock (JR) model, which constitutes an anisotropic elastic perfectly plastic constitutive model. Two orthogonal slide planes are used in correspondence with the horizontal and the vertical joints of the masonry. A Coulomb criterion is used to simulate failure in each individual plane. Failure mechanisms, such as vertical, horizontal or shear cracking, developed in the body of the superstructure, are identified.

1 INTRODUCTION

Induced earthquakes related to gas-field depletion have been striking Groningen since the 1990's. The frequency and intensity of this man-induced seismicity have been increasing since then, compelling Dutch authorities to take measures against potential structural damages and fatalities. The strongest seismic event was recorded in Loppersum on August 16th 2012, with a magnitude (M_w) of 3.6. Despite the relatively modest intensity of these seismic events, they still constitute a major concern due to the shallow hypocentre (~ 3 km below ground surface) and the particular characteristics of the uppermost soil layers.

Available geotechnical data indicate that the soil surface in Groningen consists of soft soil deposits, mostly soft clays, organics and peats, up to a depth of 10 m (Arup, 2015). These layers significantly alter the seismic ground motion leading to non-linear site effects. The groundwater table is approximately 1 m below the ground surface.

The majority of the houses in Groningen are shallow founded, commonly made of unreinforced masonry. Simplicity in construction and architectural heritage lead to structural uniformity in the wider region. No antiseismic regulations have been taken into account in the design, thus most of the masonry structures are vulnerable to seismic excitations (Arup, 2013).

The present study focuses on the influence of the shallow soft soil deposits on the strong ground motion and the subsequent response of a shallow founded masonry structure. Site specific response analyses are performed for the region of Loppersum in PLAXIS 2D (2016 version). The resulting pseudo-static acceleration (PSA) spectra at the ground surface are compared to the design spectrum provided by NPR 9998:2015. Liquefaction potential is assessed both analytically and numerically. The response of a typical Dutch masonry residence under in-plane seismic excitation (without triggering liquefaction) is investigated. Emerging failure mechanisms are identified.

2 SOIL CHARACTERISTICS

Two characteristic soil classes are encountered in Groningen, namely the "Normal site conditions" and the "Special site conditions" (Vasileiadis et al., 2015). The former conditions are applicable to the majority of Groningen region, while the latter is representative for specific areas, where organics are encountered in the top 10 m. In the present study, a design soil profile in Loppersum is used, typical of "Normal site conditions". Design material parameters are derived based on the seismic cone penetration test (SCPT) 60533 (Arup 2015).

Four soil layers are distinguished over a depth of 30 m. The topsoil layer is 8.5 m deep and consists of soft silty clay (Clay01), lying upon a 5.5 m deep silty sand (Sand01). Between 14 and 26.5 m, a stiffer silty clay is located (Clay02), below which a silty sandy layer lies up to a depth of 30 m (Sand02). Since bedrock in Groningen is located at great depth (>200 m), an apparent half-space is set at 30 m (Arup, 2015). A simplified illustration of the soil stratigraphy is presented in Figure 1(a).

Empirical correlations are used to determine soil parameters. The unit weight (γ) is derived based on Robertson & Cabal (2010). The overconsolidation ratio (OCR) of clayey deposits is estimated based on Kulhawy & Mayne (1990). OCR of sandy layers is assumed equal to 1.0. The undrained shear strength (s_u) of clayey layers is assessed by using the Stress History and Normalised

Soil Engineering Properties (SHANSEP) method (Ladd & Foott, 1974). A minimum value of 20 kPa is assumed close to the ground surface. The plasticity index (PI) is taken equal to 25%, as suggested by Arup (2015). The best estimate (BE) shear wave velocity (v_s) profile provided by Arup (2015) is adopted, presented in Figure 1(b), together with the selected design profile for the present study. The small strain shear modulus (G_0) is calculated by Equation 1, in which ρ is the soil density. An overview of the selected soil properties per layer is presented in Table 1.

$$G_0 = \rho \cdot v_s^2 \qquad [1]$$

Four different shear stiffness degradation curves are selected to model hysteretic damping in each soil layer. Stiffness degradation is modelled by means of Equation 2 (Santos & Correia, 2001). The small strain shear stiffness modulus (G_0^{ref}) at reference pressure of 100 kPa is estimated based on the calculated G_0 profile. The shear strain at which the secant shear modulus (G_s) is reduced to 72.2% of G_0^{ref} is selected such that the generated stiffness degradation curves are in close agreement to the ones provided by Arup (2015). However, the tangent shear modulus G_t is bound by a lower limit, which is imposed by the unloading-reloading shear modulus (G_{ur}) (Brinkgreve et al., 2007). The latter is calculated by Equation 3, based on the unloading-reloading Young's modulus (E_{ur}). The shear strain at which the secant shear stiffness (G_t) reaches the value of G_{ur} represents the cut-off shear strain ($\gamma_{cut-off}$) (Equation 4). Figures 2(a) to 2(d) show the adopted stiffness degradation curves for each corresponding soil layer.

$$G_s = G_0/[1 + 0.385\,(\gamma/\gamma_{0.722})] \qquad [2]$$

$$G_{ur} = E_{ur}/[2(1 + v_{ur})] \qquad [3]$$

$$\gamma_{cut-off} = (\gamma_{0.722}/0.385) \cdot \left(\sqrt{G_0/G_{ur}} - 1\right) \qquad [4]$$

The hysteretic damping ratio (ξ) is given by Equation 5, in which E_D is the dissipated energy and E_s the energy accumulated at the maximum shear strain (γ_c) during cyclic shear loading. Figures 2(e) and 2(f) illustrate the adopted curves for ξ, per soil layer.

$$\xi = E_D/(4\pi E_S) \qquad [5]$$

Apart from hysteretic damping, Rayleigh damping is assigned to all soil layers. To calibrate the Rayleigh damping coefficients α and β, a target damping ratio equal to 1% is assumed and the methodology proposed by Hudson et al. (1994) is followed. The first target frequency (f_1) is selected equal to the fundamental eigenfrequency of the soil deposit, defined as the frequency at which the most significant amplification can be expected (first mode shape). The first target frequency is given by Equation 6. The second target frequency (f_2) is calculated considering the ratio of the dominant frequency of the input time histories (estimated via the Fourier spectra) over f_1. Thus, f_1 is selected equal to 1.52 Hz (assuming an average $\overline{v}_s$ of the soil deposit equal to 183 m/s and total height H equal to 30 m) and f_2 is selected equal to 3.00 Hz.

Besides the soil properties presented in Table 1, additional soil parameters are estimated based on empirical formulae provided by Lunne et al. (1997). All selected values are presented in Tables 2 and 3.

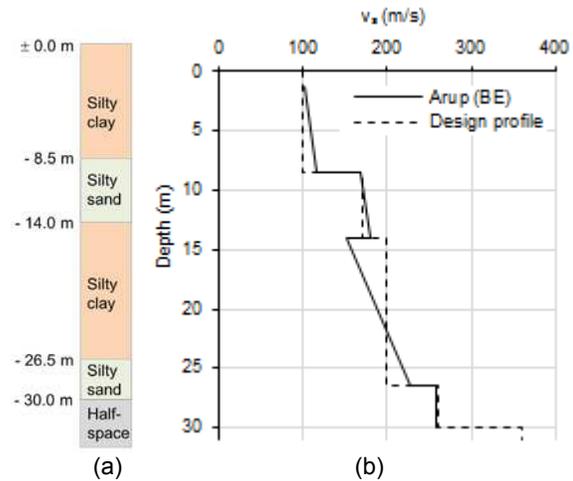$$f_1 = \overline{v}_s/(4H) \qquad [6]$$

(a)   (b)

Figure 1. Soil stratigraphy (a) and best estimate (BE) shear wave velocity profile provided by Arup (2015), and selected design profile for the present study (b).

Table 1. Soil properties per layer derived from the SCPT 60533.

Parameter	Clay01	Sand01	Clay02	Sand02
Depth (m)	0.0-8.5	8.5-14.0	14.0-26.5	26.5-30.0
γ (kN/m³)	16.0	17.5	19.0	20.0
OCR (-)	2.0	1.0	4.0	1.0
s_u (kN/m²)	20.0	-	125.0	-
PI (%)	25	-	25	-

3   SOIL CONSTITUTIVE MODELS

Clayey layers are modelled using the Generalised Hardening Soil (GHS) model, while sandy layers are modelled by means of either the GHS or the UBC3D-PLM model (Tsegaye (2010) and Petalas & Galavi (2013)), depending on the purpose of the analysis.
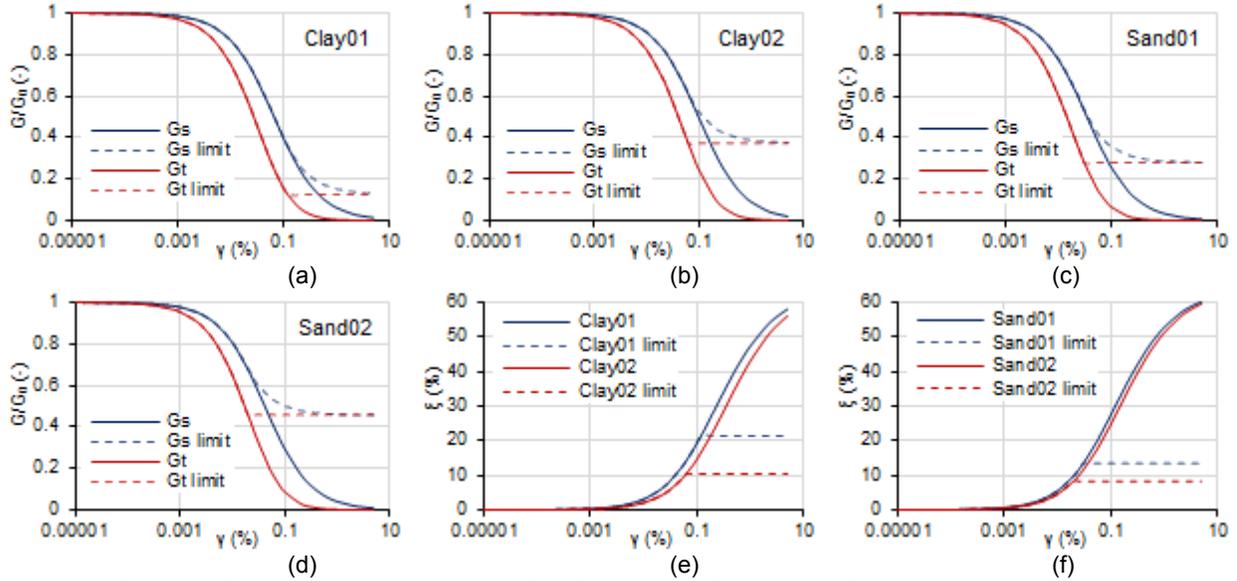
Figure 2. Shear stiffness degradation curves for Clay01 (a), Clay02 (b), Sand01 (c) and Sand02 (d), and the corresponding damping ratio curves for clay (e) and sand (f) profiles.

The GHS model is a more customised version of the original Hardening Soil model with small strain stiffness (HSsmall). It allows for different configurations of stress/strain dependency and selecting the appropriate yielding functions. The selected model parameters are presented in Table2.

Table 2. Model parameters for the GHS model.

Parameter	Clay01	Sand01	Clay02	Sand02
E_{50}^{ref} (kN/m^2)	5000	20000	12500	37500
E_{oed}^{ref} (kN/m^2)	4000	16000	10000	30000
E_{ur}^{ref} (kN/m^2)	15000	60000	37500	112500
m (-)	0.7	0.5	1.0	0.5
c'_{ref} (kN/m^2)	2.0	0.0	7.0	0.0
φ' (°)	22.0	36.0	26.0	36.0
ψ (°)	0.0	6.0	0.0	6.0
$\gamma_{0.722}$ (-)	0.00025	0.00013	0.00038	0.00016
G_0^{ref} (kN/m^2)	50000	90000	42000	120000
v'_{ur} (-)	0.2	0.2	0.2	0.2
p_{ref} (kN/m^2)	100	100	100	100
R_f (-)	0.9	0.9	0.9	0.9
σ_t (kN/m^2)	0.0	0.0	0.0	0.0
K_0 (-)	0.81	0.41	1.03	0.41

For all soil layers, the stress-dependent stiffness is kept constant during a certain calculation phase, based on the stresses at the beginning of the calculation phase. The strain-dependent stiffness is modelled in the same way as the HSsmall model, based on Equation 2. The Mohr-Coulomb failure criterion is used in combination with shear hardening, ignoring cap hardening.

The UBC3D-PLM model is used to assess liquefaction potential of sandy layers. The model is able to capture the evolution of excess pore pressures. Model parameters are derived based on Standard Penetration Tests (SPT) (Makra, 2013). Empirical formulations are used to correlate the cone resistance profile of the SCPT 60533 with normalised SPT blows $(N_1)_{60,cs}$ (Lunne et al., 1997). The selected model parameters are presented in Table 3.

The underlain half-space is modelled as Linear Elastic (LE) soil material. A moderate value of 360 m/s is adopted for the shear wave velocity. The unit weight is taken equal to 21.4 kN/m^3 (Arup, 2015).

Table 3. Model parameters for the UBC3D-PLM model.

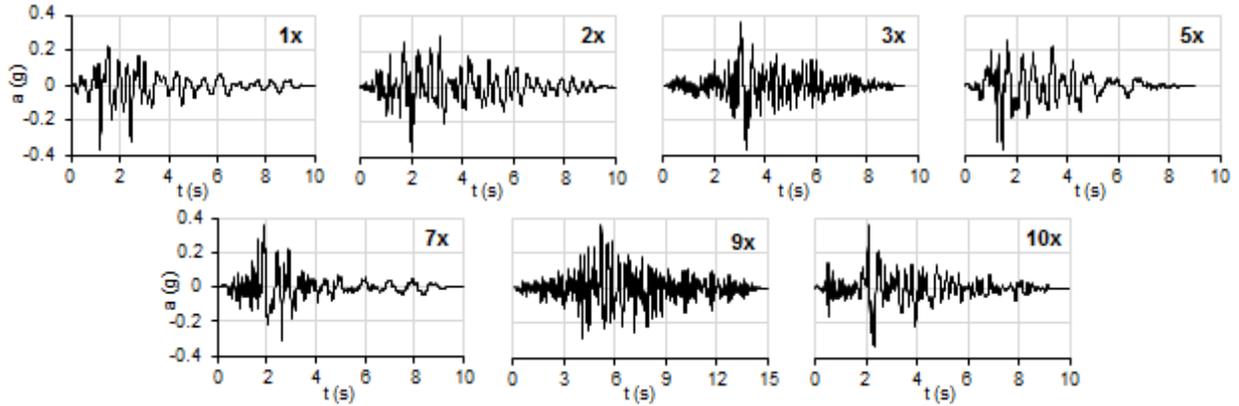| Parameter	Sand01	Sand02
φ'_{cv} (°)	35	33
φ'_p (°)	36	36
c' (kN/m^2)	0.0	0.0
k_G^e (-)	1013	1189
k_G^p (-)	593	1609
k_B^e (-)	709	832
m_e (-)	0.5	0.5
n_e (-)	0.5	0.5
n_p (-)	0.4	0.4
p_{ref} (kN/m^2)	100	100
R_f (-)	0.8	0.7
σ_t (kN/m^2)	0.0	0.0
K_0 (-)	0.41	0.41
$(N_1)_{60,cs}$ (-)	13	21
fac_{hard} (-)	1.0	1.0
fac_{post} (-)	1.0	1.0

Figure 3. Selected input time histories from the database of NPR 9998:2015, linearly scaled to a *PGA* of 0.36 g.

4   INPUT GROUND MOTIONS

Figure 4 illustrates the location-dependent peak ground accelerations (*PGA*) at ground level, with a 10% chance of exceedance in 50 years, which corresponds to a 475-year return period (Dost & Spetzler, 2015). A magnitude (M_w) of 5 is assumed an upper bound for the induced seismicity in Groningen (Dost et al., 2013). The *PGA* values presented in Figure 4 correspond to an Importance Factor (γ_I) equal to 1.0. The highest value is 0.36 g at Loppersum.

In total eleven time histories are provided by NPR 9998:2015 for non-linear dynamic time analysis. All are spectrally matched to the 2016 NPR target design spectrum at 30 m depth. For the scope of this study, seven time histories are selected (Figure 3) and linearly scaled to a *PGA* of 0.36 g (Loppersum). The adopted code names are based on the corresponding name of each signal as provided by NPR 9998:2015, i.e. 1x, 2x etc.
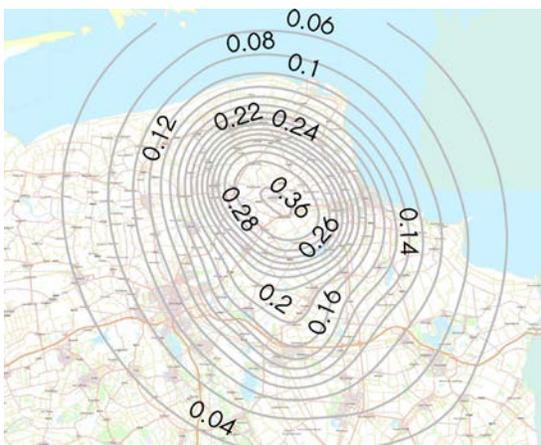

Figure 4. Hazard map of Groningen indicating the maximum expected *PGA* values at ground level for a 475-year return period (NPR 9998:2015).

5   SITE RESPONSE ANALYSIS AND LIQUEFACTION ASSESSMENT

Site response analyses (SRA) are performed in order to study the response of the soil column during seismic excitation and evaluate liquefaction potential. Since the accelerations currently recorded at the ground surface in Groningen are relatively small (< 0.1 g), phenomena of non-linearity are not yet observed (Spetzler & Dost, 2016). Nonetheless, the present study focuses on seismic events of higher intensity than the ones reported so far. The time histories depicted in Figure 3 are used as input ground motions with *PGA* equal to 0.36 g. A 31 m soil column is modelled under plane strain conditions. The width of the model is selected equal to 0.7 m in order to have an average length of the mesh elements sides less than one-eighth of the input wavelength (Kuhlemeyer & Lysmer, 1973).

The soil layers presented in Figure 1 are modelled by means of the GHS (clay layers, Table 2) and the UBC3D-PLM (sand layers, Table 3) material models. The bottom one meter is used to represent half-space by using a LE soil model. Water table is set at 1 m depth. The side boundary conditions are set to "Tied degrees of freedom". A "Compliant base" is used at the bottom of the model to apply the input ground motions, considering half the amplitude, i.e. only the upward propagating motion of the shear waves.

Numerical results in terms of the excess pore water pressure ratio r_u are presented in Table 4. Results indicate liquefaction in the top sand layer "Sand01" ($r_u \approx 1$), while such condition is not met for the bottom sand layer "Sand02" ($r_u < 1$).

Liquefaction potential of both sand layers is also evaluated analytically. The semi-empirical method proposed by Boulanger & Idriss (2014) is used. The value of the peak horizontal acceleration at ground surface (α_{max}) is estimated by site response analyses, in which excess pore pressures (i.e. liquefaction potential) and undrained behaviour are not considered. This is done by using the GHS model for all clay and sand soil layers (Table 2). All seven time histories presented in Figure 3 are used, with *PGA* equal to 0.36 g ($\alpha_{max,in}$). Input signals are applied at 31 m depth. Results in terms of output *PGA* values at ground surface ($\alpha_{max,surf}$) and amplification factor

(*A*) of $\alpha_{max,surf}$ over $\alpha_{max,in}$ are given in Table 5. The obtained factor of safety (*FoS*) against liquefaction is presented as well. All input seismic signals result in liquefaction of the top sand layer "Sand01" (*FoS*<1.2), while the bottom sand layer "Sand02" is found to be safe against liquefaction (*FoS*>1.2).

Table 4. Results of numerical liquefaction assessment for all considered input seismic signals (Figure 3).

Parameter	1x	2x	3x	5x	7x	9x	10x
$r_{u,\,Sand01}$ (-)	0.97	0.98	0.99	0.98	0.98	1.00	0.97
$r_{u,\,Sand02}$ (-)	0.18	0.20	0.19	0.26	0.23	0.19	0.27

Table 5. Results of analytical liquefaction assessment for all considered input seismic signals (Figure 3).

Parameter	1x	2x	3x	5x	7x	9x	10x
$\alpha_{max,in}$ (g)	0.36	0.36	0.36	0.36	0.36	0.36	0.36
$\alpha_{max,surf}$ (g)	0.25	0.31	0.27	0.26	0.24	0.26	0.27
A (-)	0.70	0.87	0.74	0.73	0.65	0.72	0.74
FoS $_{Sand01}$	0.5	0.4	0.5	0.5	0.5	0.5	0.5
FoS $_{Sand02}$	1.6	1.3	1.5	1.5	1.6	1.5	1.5

As presented in Table 5, input *PGA* at 30 m depth is deamplified due to the soft soil deposits (*A* < 1.0), if a non-liquefiable state is assumed (sand layers are modelled with the GHS model). Due to the impedance contrast between the soft shallow layers and the stiffer sublayers, the predominant natural frequency and the maximum amplitude of the shear seismic waves which propagate upwards are modified. Vasileiadis et al. (2015) and Pruiksma (2016) performed non-linear SRA and concluded that, for "Normal site conditions", de-amplification occurs in the short period band (0.2s<*T*<0.8s), while amplification is observed in the long period band (0.8s<*T*<2.0s). The soundness of the finite element calculations for the whole period band is checked considering the analyses in which the GHS model is used for sand and clay soil layers. Figure 5(a) presents the obtained response spectral accelerations at the ground surface (for structural damping ratio *ξ*=5%) and Figure 5(b) the corresponding spectral ratio (input over output spectral accelerations), for all considered input time histories with *PGA* equal to 0.36 g. In Figure 5(a), the design spectrum (DS) provided by NPR 9998:2015 is plot as well. As observed, the numerical results match very well the design spectrum. In addition, deamplification of the input ground motion in the short period band and amplification in the long period band are well-captured.

6   MODEL FOR MASONRY STRUCTURES

The use of the Jointed Rock (JR) model is adopted in this study in order to simulate unreinforced masonry structures. The JR model constitutes an anisotropic

elastic perfectly plastic constitutive model. The model is originally used to simulate the behaviour of stratified and jointed rock layers. A maximum of three sliding planes with different strength properties may be considered. In each individual plane, plastic yielding is formulated by means of the Coulomb failure criterion. In this study, two orthogonal slide planes are used, which represent the horizontal and the vertical joints of the masonry accordingly.
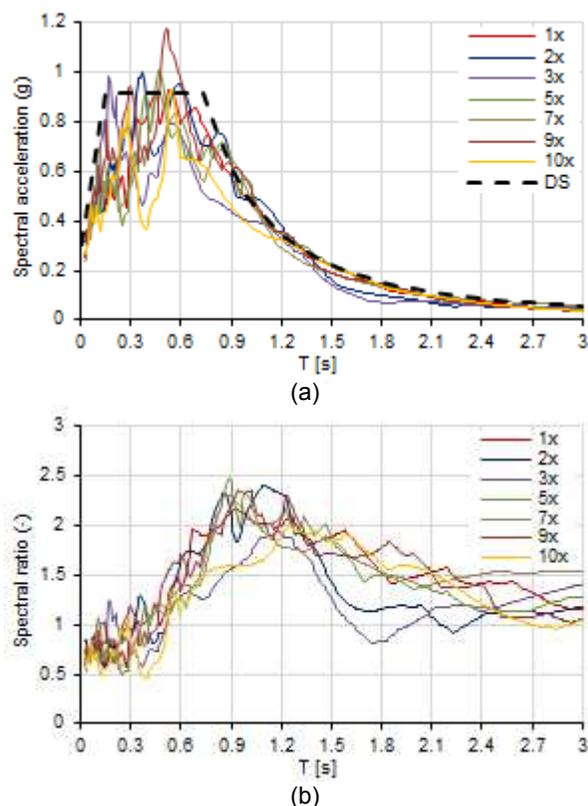

(a)

(b)

Figure 5. Spectral acceleration at ground surface for seven input time histories with *PGA* equal to 0.36 g and structural damping ratio *ξ*=5% (a) and spectral ratio between input (half-space) and output (ground surface) spectral acceleration spectra.

The homogenisation method proposed by de Felice et al. (2010) is used to form the elastic response. The elastic moduli E_1 and E_2 in horizontal and vertical directions are given by Equation 7, in which E_b is the Young's modulus of the blocks (bricks), E_m is the Young's modulus of the mortar, *h* and *b* are the average height and width of the blocks, *t* is the average thickness of the mortar and v_m the Poisson's ratio of the mortar. Table 6 presents the selected physical (Michalaki, 2015) and mechanical (NPR 9998:2015) properties of the masonry structure, while Table 7 gives the resulting material properties for the JR model. Subscript "*1*" refers to horizontal direction while Subscript "*2*" refers to vertical direction. Poisson's ratio (*v*) in both directions is taken equal to zero to approximate plane stress conditions.

$$\frac{1}{E_1} = \frac{1}{E_b} + \frac{8ht(1 - v_m^2)}{b^2 E_m (1 - v_m)} \ ; \ \frac{1}{E_2} = \frac{1}{E_b} + \frac{t(1 - v_m^2)}{h E_m} \qquad [7]$$

Table 6. Physical and mechanical properties of the masonry structure (after Michalaki (2015) and NPR 9998:2015).

Parameter	Symbol	Value	Unit
Density	ρ	1.92	t/m³
Young's modulus (block)	E_b	$5.0 \cdot 10^6$	kN/m²
Young's modulus (mortar)	E_m	$1.0 \cdot 10^6$	kN/m²
Poisson's ratio (mortar)	v_m	0.20	-
Block height	h	0.06	m
Block width	b	0.20	m
Mortar thickness	t	0.01	m

Table 7. Model parameters for the JR model.

Parameter	Symbol	Value	Unit
Unit weight	γ	19.2	kN/m³
Young's modulus (horizontal direction)	E_1	$2.91 \cdot 10^6$	kN/m²
Young's modulus (vertical direction)	E_2	$2.78 \cdot 10^6$	kN/m²
Cohesion	$c_{1,2}$	50.0	kN/m²
Friction angle	$\varphi_{1,2}$	37.0	°
Dilatancy	$\psi_{1,2}$	0.0	°
Tensile strength (horizontal direction)	$f_{tens,1}$	80.0	kN/m²
Tensile strength (vertical direction)	$f_{tens,2}$	50.0	kN/m²

7   CASE STUDY

A case study is presented, considering a typical Dutch (unreinforced) masonry residence located at Loppersum (Michalaki, 2015). The building is modelled by means of the JR model as discussed in the previous section. Two steel braces are placed above the openings to contribute to stiffness, modelled as elastic beams. Horizontal line loads are applied to the first and second floor levels to represent active and dead (floor slabs, roof) loads. The assigned values are 1.5 and 1.7 kN/m/m respectively. A concrete slab is placed beneath the superstructure to simulate its shallow foundation. Linear elastic non-porous material is used. Figure 6(b) illustrates the masonry structure.

Purpose of this study is to evaluate the performance of the superstructure under in-plane seismic excitation, without triggering liquefaction. Such scenario is thought to be more critical for the superstructure. Thus, a lower input *PGA* equal to 0.18 g is used, with return period approximately equal to 100 years (Arup, 2016). Liquefaction potential is assessed analytically and numerically. In both ways it is proven that liquefaction of the top sand layer does not occur.

Figure 7 illustrates the results of the SRA analyses in terms of spectral accelerations at the ground surface (structural damping ratio ξ=5%). Only the results of the input seismic motion "*2x*" are displayed as a characteristic case. In this figure a comparison between the GHS and the UBC3D-PLM under non-liquefiable conditions is attempted. As it can be seen, GHS model damps out accelerations more than UBC3D-PLM, especially in the period band between 0.3 and 0.8 s, falling well below the design spectrum (DS) of NPR 9998:2015. The opposite occurs for periods between 0.8 and 1.5 s. Hysteretic damping is formulated different in the GHS and UBC3D-PLM models. The GHS model follows the same methodology adopted in the HSsmall model (Brinkgreve et al., 2007). In the UBC3D-PLM model the plastic shear modulus is formulated as a function of the number of cycles during dynamic loading (Petalas & Galavi, 2013). In the present example, it is thought that the GHS model offers better approach of the actual hysteretic damping as the shear stiffness degradation curves have been determined based on in-situ soil data. Thus, the GHS model is used to simulate all soil layers for this case study.

A plane strain model is used. The soil profile depth equals 31 m, similar to the SRA analysis discussed above. Side model boundaries are extended to account for geometrical damping, resulting in a model 180 m wide. Water table is set at 1 m depth. The side boundary conditions are set to "Free field", while a "Compliant base" is used at the bottom of the model. Figure 6(a) depicts part of the model and the generated mesh at the vicinity of the masonry structure.

The initial stress state is generated with plastic analysis by assuming drained conditions (consolidated state of soils). Undrained conditions are taken into account for the dynamic analysis.

Free vibration analysis is performed to determine the eigenfrequency of the first two modes of the superstructure, resulting in f_{1m} equal to 0.67 Hz and f_{2m} equal to 2.00 Hz. Rayleigh damping coefficients for the masonry structure are selected such that 5% damping corresponds to 0.67 Hz (f_{1m}) and 3.00 Hz (correlation between f_{2m} and the predominant frequency of input time histories).

Only the results of the dynamic analysis in case of the seismic signal "2x" are discussed, as a characteristic example of all the analyses performed. Failure of the superstructure is identified in terms of crack patterns. Figure 8(a) depicts the developed plastic points at the end of the dynamic calculation. It is apparent that the left and center piers of the ground floor suffer from extensive damage. Significant amount of plastic points is also observed at the spandrel wall. Crack patterns become more apparent by inspecting the total deviatoric strains (Figure 8(b)). Deviatoric strains with maximum value around 0.3% occur at the spandrel wall indicating shear cracking (sliding). Horizontal cracks are primarily observed at the left and centre pier of the structure. The part of the wall below the ground floor opening suffers from horizontal and vertical cracking as well.
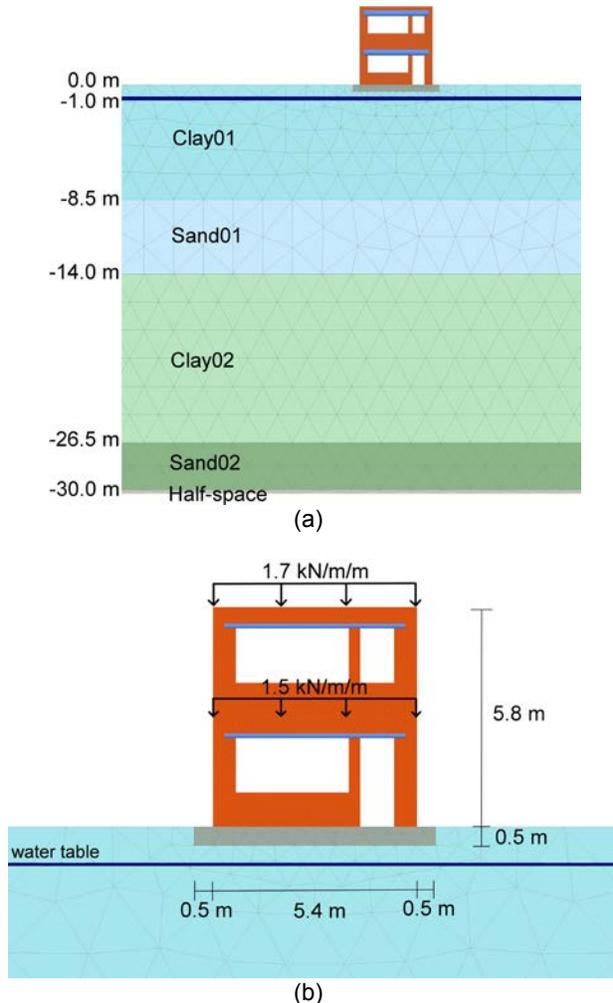
(a)   (b)

Figure 8. Plastic points (red coloured areas) (a) and total deviatoric strains (b) in the superstructure.

(a)

(b)

Figure 6. Model geometry and finite element mesh for the case study (a) and close-up of the superstructure (b).

8   CONCLUDING REMARKS
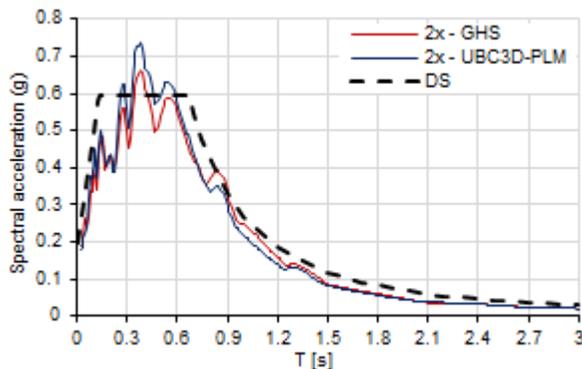
SRA analyses were performed in the finite element program PLAXIS 2D (2016 version) for a soil profile in Groningen (Loppersum), the Netherlands. Seven input ground motions were used, scaled to a *PGA* of 0.36g. The UBC3D-PLM model was employed to assess liquefaction potential of sand layers. Numerical results were found to be in agreement with the analytical evaluation, indicating that the top sand layer of the considered soil profile is susceptible to liquefaction. Under the same seismic intensity, the non-linear response of the soft soil deposits was investigated by modelling all soil layers with the GHS model. The nonlinear phenomena caused by the nature of top soft soil layers were well-captured.

A case study of a typical Dutch masonry residence is presented as well. The superstructure is modelled by means of the JR model. The *PGA* of the input time histories is scaled to 0.18 g in order to investigate the response of the structure under a non-liquefiable state. Numerical results in terms of plastic points and deviatoric strains indicate shear failure of piers and walls.

9   REFERENCES

Arup (2013). *NAM, Groningen 2013, Preliminary Structural Upgrading Strategy for Groningen*. Arup report 229746, Amsterdam, the Netherlands.

Arup (2015). *Groningen Earthquakes Structural Upgrading, Site Response Analysis*. Arup report 229746, Amsterdam, the Netherlands.

Arup (2016). *Groningen Earthquakes Structural Upgrading, Risk Assessment of Falling Hazards in Earthquakes on the Groningen region: Appendices 1-4*. Arup report 229746, Amsterdam, the Netherlands.

Boulanger, R.W., and Idriss, I.M. (2014). CPT and SPT based liquefaction triggering procedures. *Center for Geotechnical Modeling, Department of Civil and Environmental Engineering, University of California, Davis,* CA. Report No. UCD/CGM-14/01.

Brinkgreve, R.B.J. and Kappert, M.H. and Bonnier, P.G. (2007). Hysteretic damping in a small-strain stiffness model. In *Proc. 10th Int. Symp. Numer. Mod. Geomech.*, Rhodes, Greece, 737-742.

Figure 7. Spectral acceleration at ground surface for the input time history "2x" with *PGA* equal to 0.18 g and structural damping ratio ξ=5%.
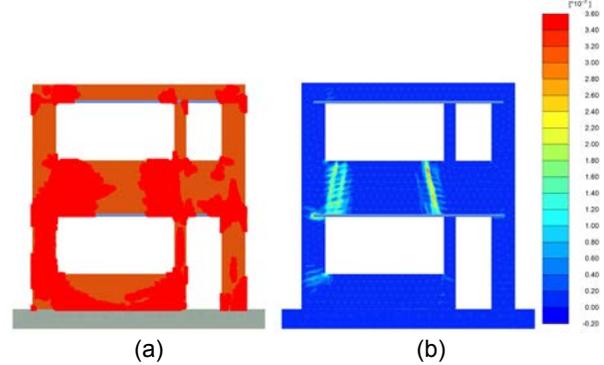
de Felice, G. and Amorosi, A. and Malena, M. (2010). Elasto-plastic analysis of block structures through a homogenization method. *Int. J. Numer. Analyt. Methods Geomech.*, 34(3):221-247.

Dost, B. and Caccavale, M. and van Eck, T. and Kraaijpoel, D. (2013). *Report on the expected PGV and PGA values for induced earthquakes in the Groningen area*. KNMI report, KNMI, the Netherlands.

Dost, B. and Spetzler, J. (2015). *Probabilistic Seismic Hazard Analysis for Induced Earthquakes in Groningen*. KNMI report, KNMI, the Netherlands.

Hudson, M. and Idriss, I.M. and Beikae, M. (1994). User's manual for QUAD4M. *Center for Geotechnical Modeling, Department of Civil and Environmental Engineering, University of California, Davis*, California, USA.

Kuhlemeyer, R.L. and Lysmer, J. (1973). Finite element method accuracy for wave propagation problems. *J. Soil Mech. and Found. Dev.*, 99(5):421–427.

Kulhawy, F.H. and Mayne, P.W. (1990). Manual on Estimating Soil Properties for Foundation Design. *Cornell University, Geotechnical Engineering Group, Hollister Hall, EL-6800, Research Project 1439-6,* Ithaca, NY.

Ladd, C.C. and Foott, R. (1974). New Design Procedure for Stability of Soft Clay. *J. Geotech. Eng. Div.*, ASCE, 100(7):763-786.

Lunne, T. and Robertson, P.K. and Powell, J.J.M. (1997). *Cone Penetration Testing in Geotechnical Practice.* Spon Press, Taylor & Francis Group, London and New York.

Makra, A. (2013). Evaluation of the UBC3D-PLM constitutive model for prediction of earthquake induced liquefaction on embankment dams*. MSc thesis, Department of Civil Engineering and Geosciences, Delft University of Technology*, Delft, the Netherlands.

Michalaki M. (2015). Seismic Assessment of a Typical Dutch Rijtjeshuis. *MSc thesis, Department of Civil Engineering and Geosciences, Delft University of Technology*, Delft, the Netherlands.

NPR 9998:2015 (2015). *Beoordeling van de constructieve veiligheid van een gebouw bij nieuwbouw, verbouw en afkeuren – Grondslagen voor aardbevingsbelastingen: geïnduceerde aardbevingen*. Nederlands Normalisatie Instituut, the Netherlands.

Petalas, A. and Galavi, V. (2013). *Plaxis liquefaction model UBC3d-PLM*. Plaxis bv, Delft, the Netherlands.

Pruiksma, J.P. (2016). *Nonlinear and Equivalent Linear Site response analysis for the Groningen area*. TNO report, R10460, Delft, the Netherlands.

Robertson, P.K. and Cabal, K.L. (2010). Estimating soil unit weight from CPT. In *Proc. 2nd Int. Symp. Cone Pen. Test.*, CA, USA. Paper No. 40.

Santos, J. A. and Correia, A. G. (2001). Reference threshold shear strain of soil. Its application to obtain an unique strain-dependent shear modulus curve for soil. In *Proc. 15th Int. Conf. on Soil Mech. and Geotech.Eng.,* Istanbul, Turkey, 1:267-270.

Spetzler, J. and Dost, B. (2016). *Probabilistic Seismic Hazard Analysis for Induced Earthquakes in Groningen, Update June 2016*. KNMI report, KNMI, the Netherlands.

Tsegaye, A.B. (2010). *PLAXIS liquefaction model. Appropriation, Elaboration, Implementation, Verification*. Plaxis bv, Delft, the Netherlands.

Vasileiadis, M. and Go, J. and Lubkowski, Z. and Grant, D. and de Vries, R. (2015). *Groningen Earthquakes Structural Upgrading*. Technical Note 229746, Arup, London, UK.